J Mater Sci (2007) 42:2745–2752
DOI 10.1007/s10853-006-1362-3

Interfacial mechanical properties of TiN coating on steels by indentation

Shi-Yung Chiou · Dershin Gan

Received: 2 October 2005 / Accepted: 27 February 2006 / Published online: 9 January 2007

Abstract The elastic theory of indentation on nitride films/steel systems showed distribution of stresses (shear stress, radial stress and circumferential stress) near the interface and in the film. The difference in values for each stress along the distance to the load center increased with increasing Poisson's ratios of steels. The shear stresses (σ_{rz}) had the maximum value at a distance to the load center and the difference became more significant with increasing Poisson's ratios of steel substrates (from 0.2–0.3 of Poisson's ratio for high-speed steels to 0.3–0.35 for stainless steels), which accounted for the large amount of cracks inside the indent cavity of nitride films/stainless steel in spite of the smoothness outside the cavity. The calculation of σ_r and σ_z showed that the differences in nitride films/steel stress increased with increasing Poisson's ratios of steels, which also facilitated the formation of ring cracks in the film of nitride films/stainless steel composite. Indentation examination revealed the large amount of cracks inside the indent cavity of nitride film/stainless steel but smooth surface outside the cavity. These were formed under the high sinusoidal shear stress and circumferential radial stress due to the higher Poisson's ratio of stainless steel and the plastic deformation due to the lower yield stress of stainless steel (SS), which induced more local residual stresses, whereas some cracks or spalling observed around the cavity and no cracks inside the cavity were attributed to the edge effect when the conical indenter strained the surface downward for nitride film/high-speed steel (HSS) system.

S.-Y. Chiou (✉)
Department of Mold and Die Engineering,
National Kaohsiung University of Applied Science,
Kaohsiung 807, Taiwan, ROC
e-mail: sychiou@cc.kuas.edu.tw

D. Gan
Institute of Materials Science and Engineering,
National Sun Yat-Sen University,
Kaohsiung 80424, Taiwan, ROC

Introduction

The performance and reliability of hard film on tool material are often limited by its mechanical integrity and its adhesion to the substrate. The adhesion is related to the interfacial strength between the film and substrate which is controlled by some important parameters such as the film/substrate mismatch, the flaw distribution in the film and at the film/substrate interface, the residual stress in the film and the imposed stress. The indentation technique, used early to measure the indentation fracture of ceramics [1–4] and interfacial shear strength of the ceramic–ceramic interface [5–9], is becoming a common method for evaluating the interfacial mechanical properties of hard film–hard substrate and adhesion properties of hard film/tool steel due to its ease of operation and analysis [10–12].

The elastic theory of indentation on ceramics showed the distribution of stresses [1, 2]. The indentation crack initiation and propagation, relationship between indentation damage, residual stresses and mechanical properties such as hardness, toughness were described by elastic/plastic fields [3, 4]. The hardness, stresses, crack evolutions and adhesion of

coatings on brittle substrate were analyzed using on elastic/fracture mechanics coupled with indentation examinations.

The effect of plasticity of the metal substrate and the edge effect on the interfacial strength of ceramic/metal system were studied by Evans et al. [13–16]. They demonstrated that metal plasticity can be either beneficial due to the plastic blunting of interfacial cracks or detrimental due to the residual stresses created around cracks in the ceramic film and the stress concentration at the edge. The shear strengths of ceramic/metal interface were also described with the same model. Quantitative relationship between the crack density and the elastic and plastic parameters, together with experimental observations of interface cracks was conducted by Agrawal [17, 18]. However, the indentation technique for hard films/substrate was expected to work well only when the shear strength of interface is less than the yield strength of the matrix. The evaluations of indentation for hard film/steel systems in this study were carried out by examining the surface and cross-section indentation fracture patterns with different steel substrates combined with elastic analysis and elastic/plastic model previously described.

Experimental

The depositions of titanium nitride films were carried out with a DC magnetron reactive sputtering system. Before deposition, all specimens were mechanically polished down to 1,000 grade emery paper and ultrasonically cleaned with alcohol and acetone for 15 min each.

The discharge power was 220 watts and substrate temperature was kept at 300 °C. The argon and nitrogen flow rate during the deposition were 28 sccm and 3.1 sccm, respectively, with a specific ratio of 9.3. The working pressure of the chamber was kept at 0.8 Pa. Pre-sputtering of 15 min was normally performed by plasma to clean the target surface while pre-sputtering of 5 min was taken for comparison. The deposition time was 1 h for growing films to about 2 μm thick, with the first 5 min for growing the metallic Ti interlayer.

Pure titanium (99.99% purity) was used as sputtering targets for deposition. The nitride films of TiN were deposited on AISI M2 high-speed steels (HSS) which were quenched and tempered to a hardness of HV 780 (HRC63). Some nitride films were deposited on type 304 stainless steels (SS) for comparison. The α-step method and X-ray diffraction were used to determine the thickness and phases of TiN films.

Indentation method was used to investigate the adhesion properties of coatings in this study. Prior to the experiments, theoretical analysis of stress distribution and stress–strain relationship were established by the elastic theory. Indentation tests for nitride film-coated steels were conducted with a Rockwell Hardness Tester using a conical diamond indentor and a 150 kg loading force. Optical microscope (OM) and scanning electron microscope (SEM) were used to examine the indented patterns of the top view and cross-section.

Results

Elastic analysis of indentation for nitride/steel systems

The stress distribution of steel coated with hard film by indentation is shown as an elastic half-space subjected to a normal point load P, as seen in Fig. 1. The elastic solutions are:

$$\sigma_r = 2\mu B\left[\frac{Z^2}{R^3(Z+R)} - \frac{\rho^2}{R^2(Z+R)^2}\right] + 2\mu A\left[\frac{-3\rho^2 Z}{R^5} - \frac{}{R^3(\lambda+\mu)}\right] \quad (1)$$

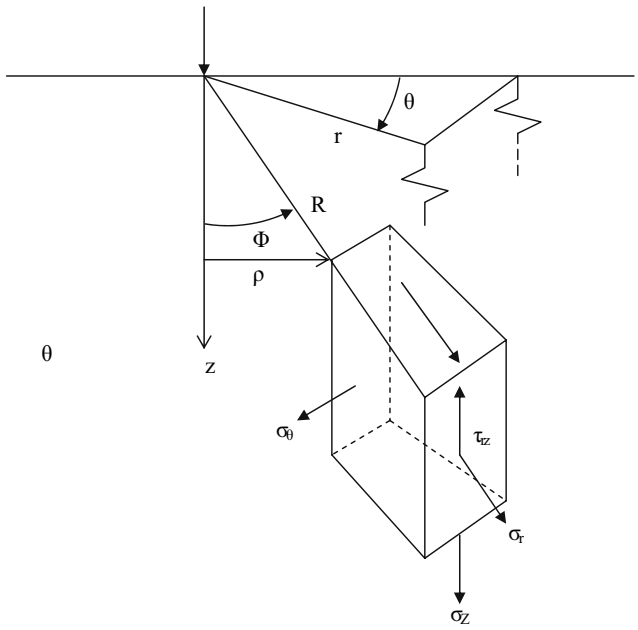

Fig. 1 Coordinate system and stress components for indentation testing

$$\sigma_\theta = 2\mu B\left[\frac{Z^2+\rho^2}{R^3(Z+R)}\right] + 2\mu A\left[\frac{\mu Z}{R^3(\lambda+\mu)}\right] \quad (2)$$

$$\sigma_Z = 2\mu B\frac{Z}{R^3} + 2\mu A\left[\frac{-3Z^3}{R^5} - \frac{\mu Z}{R^3(\lambda+\mu)}\right] \quad (3)$$

$$\tau_{rz} = -2\mu B\frac{\rho}{R^3} + 2\mu A\left[\frac{-3^3}{R^5} - \frac{\mu\rho}{R^3(\lambda+\mu)}\right] \quad (4)$$

$$F = \frac{4\pi\mu A(\lambda+2\mu)}{\lambda+\mu} + 4\pi\mu B \quad (5)$$

where λ and μ are Lame constants. Z is the depth from the surface. From Fig. 1, the following equations are apparent:

$$R^2 = Z^2 + \rho^2 \quad (6)$$

$$Z = R\cos\phi \quad (7)$$

$$\rho = R\sin\phi \quad (8)$$

For the nitride film/steel substrate systems in this study, the boundary conditions are defined as follows:

(1) $Z = t$, $w_1 = w_2$
(2) $Z = t$, $\sigma_{z1} = \sigma_{z2}$
(3) $Z = 0$, $\tau_{rz} = 0$
(4) $Z = 0$, result force = F

where t is the thickness of the film and w is the displacement. The symbol 1 denotes the substrate while 2 indicates the film. For $Z = 0$, $\tau_{rz} = 0$ on the free surface, B_1 is calculated to be

$$B_1 = \frac{-A_1\mu_1}{\lambda_1+\mu_1} \quad (9)$$

Since the total force F on the surface is

$$F = \frac{4\pi\mu_1 A_1(\lambda_1+2\mu_1)}{\lambda_1+\mu_1} + 4\pi\mu_1 B_1 \quad (10)$$

A_1, B_2 can be solved to be

$$A_1 = \frac{F}{4\pi\mu_1}, {}_1 = \frac{-F}{4\pi(\lambda_1+\mu_1)} \quad (11)$$

Similarly, from $Z = t$, $\sigma_{z1} = \sigma_{z2}$, A_2, B_2, K_1 and K_2, can be solved to be

$$A_2 = F(\lambda+\mu_2)\{\lambda_1[R^2\mu_2 + t^2(3\mu_1+\mu_2) + \mu_1[2R^2\mu_2 + t^2(3\mu_1+\mu_2)]\}/[4\pi\mu_1(\lambda_1+\mu_1)\mu_2(\lambda_2R^2 + 4\lambda_2t^2 + 2R^2\mu_2 + 4t^2\mu_2)] \quad (12)$$

$$B_2 = \frac{FR^6(\lambda_2+\mu_2)(K_1-K_2)}{4\pi t(\lambda_2R^2 + 4\lambda_2t^2 + 2R^2\mu_2 + 4t^2\mu_2)} \quad (13)$$

$$K_1 = \frac{-\left[t^2 + \frac{R^2(\lambda_1+2\mu_1)}{\lambda_1+\mu_1}\right]\left[\frac{-3t^3}{R^5} + \frac{t\mu_2}{R^3(\lambda_2+\mu_2)}\right]}{R^3\mu_2} \quad (14)$$

$$K_2 = \frac{-3t^3\left[t^2 + \frac{R^2(\lambda_2+3\mu_2)}{\lambda_2+\mu_2}\right]}{R^3\mu_2} \quad (15)$$

In the case of the nitride/steel systems, the elastic analysis results of the radial and circumferential stresses (σ_r, σ_θ) in the film and the shear stresses at the interface (τ_{rz}) are shown in Fig. 2a–c. Figure 2a and b are the distribution of σ_r and σ_θ, respectively, at the interface as a function of φ with different Poisson's ratios of substrates. Figure 2c is the sinusoidal shear stress at the interface with different Poisson's ratios of substrates. The stress distribution curves from the film surface to interface are shown in Fig. 3a–c, which show clearly that maximum stresses are reached at the interface. Furthermore, the different indentation properties between nitride/HSS and nitride/SS specimens may be correlated with elastic/plastic analysis of indention test. The tensile fracture patterns of the nitride/SS and nitride/HSS on the surfaces of tensile-tested specimens are shown in Fig. 4a, b. The different spacing of the almost parallel cracks normal to the stress may be used to evaluate the shear stresses at the interface for each bonding system by the following equation [18]:

$$\tau_{max} = \frac{k\delta\sigma_f}{\lambda_{max}} \quad (16)$$

where δ, λ_{max} and k are, respectively, the thickness of the film, the maximum crack spacing in the region of constant crack density, and a proportional constant which varies from 2 to 6. The value of σ_f was calculated from

$$\sigma_f = E\varepsilon_f \quad (17)$$

where ε_f is the fracture strain which can be determined by the calibrated curve of crack density.

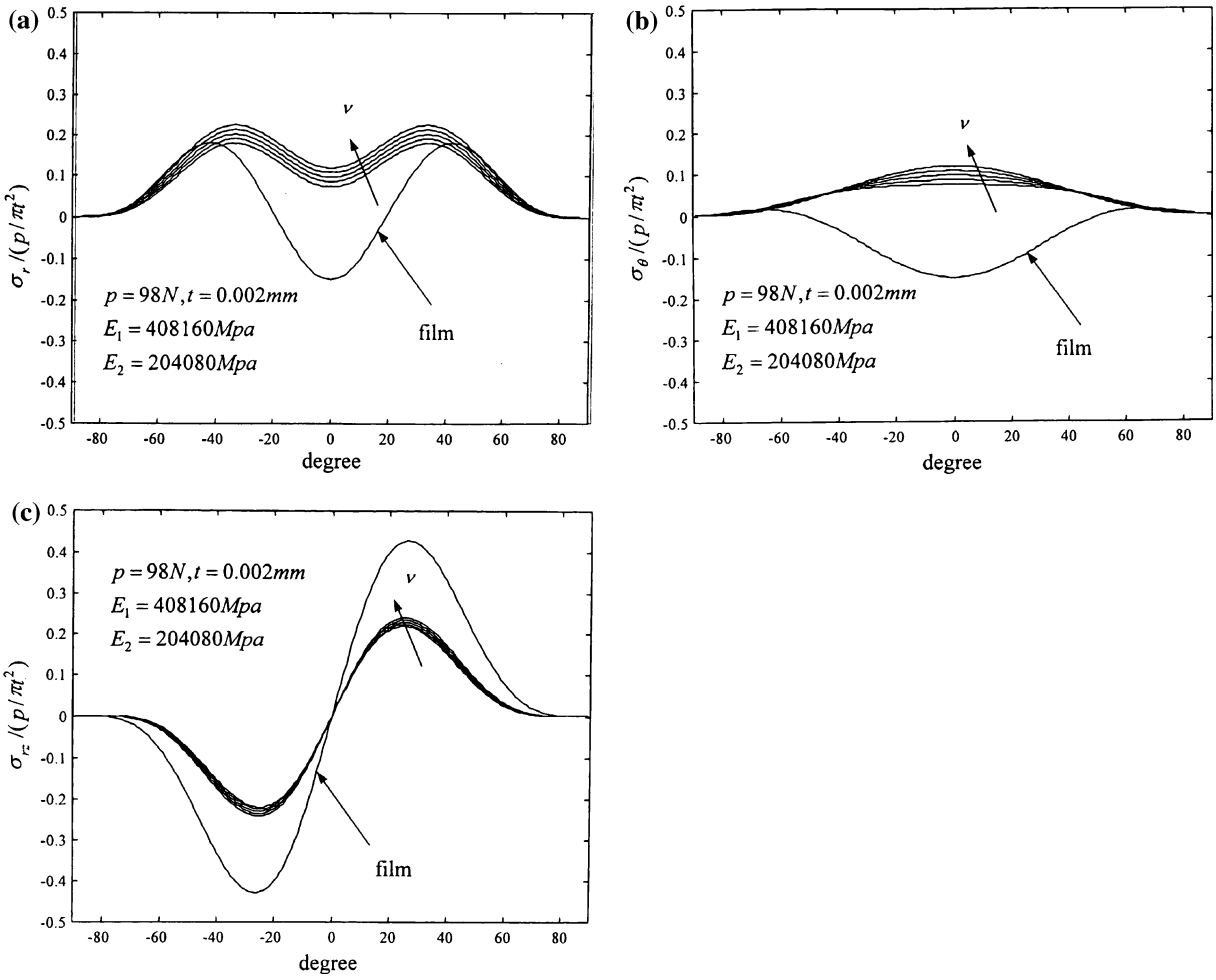

Fig. 2 (**a**) Variation in σ_r at the film/substrate interface as a function of ψ. (**b**) Variation in σ_θ at the film/substrate interface as a function of ψ. (**c**) Variation in σ_{rz} at the film/substrate interface as a function of ψ

Indentation fracture patterns

The indentation tests using a 150 kg load in a Rockwell Hardness Tester with a conical diamond indenter generally show fracture patterns as radial cracks and spalling in the area outside the indented contact cavities, which are measured by SEM. For a nitride/HSS system, either no cracks or only a small amount of short radial cracks are observed, as in Fig. 5a, indicating good nitride/HSS bonding or many lateral cracks and spallings are observed, as in Fig. 5b, indicating nitride/HSS poor bonding. However, although the top view in Fig. 5c shows no cracks, the cross-section view in Fig. 6a of nitride/SS system shows significant amount of ring cracks, lateral cracks and even some spalling inside the cavity. The cross-section view of nitride/HSS in Fig. 6b, shows a much smoother surface than those of nitride/SS due to the harder substrate. Furthermore, there are fewer cracks or spalling inside the cavity although the deformation of columnar nitride film is apparent on the inclined cavity surface as in Fig. 6c. The X-ray diffraction (XRD) results of TiN coating as shown in Fig. 7 indicate the TiN phases with the main diffraction peaks of (111) and (200) orientation which agree with other studies [19–21].

Discussion

Elastic analysis

The distributions of radial (σ_r), circumferential (σ_θ) and shear (τ_{rz}) stresses with horizontal and vertical distances from the loading center are analyzed by the elastic theory. In Fig. 1, σ_z is designated as positive in the downward direction. The maximum variations in σ_r and σ_θ between coating and substrate occur at the loading center, especially for substrate of larger

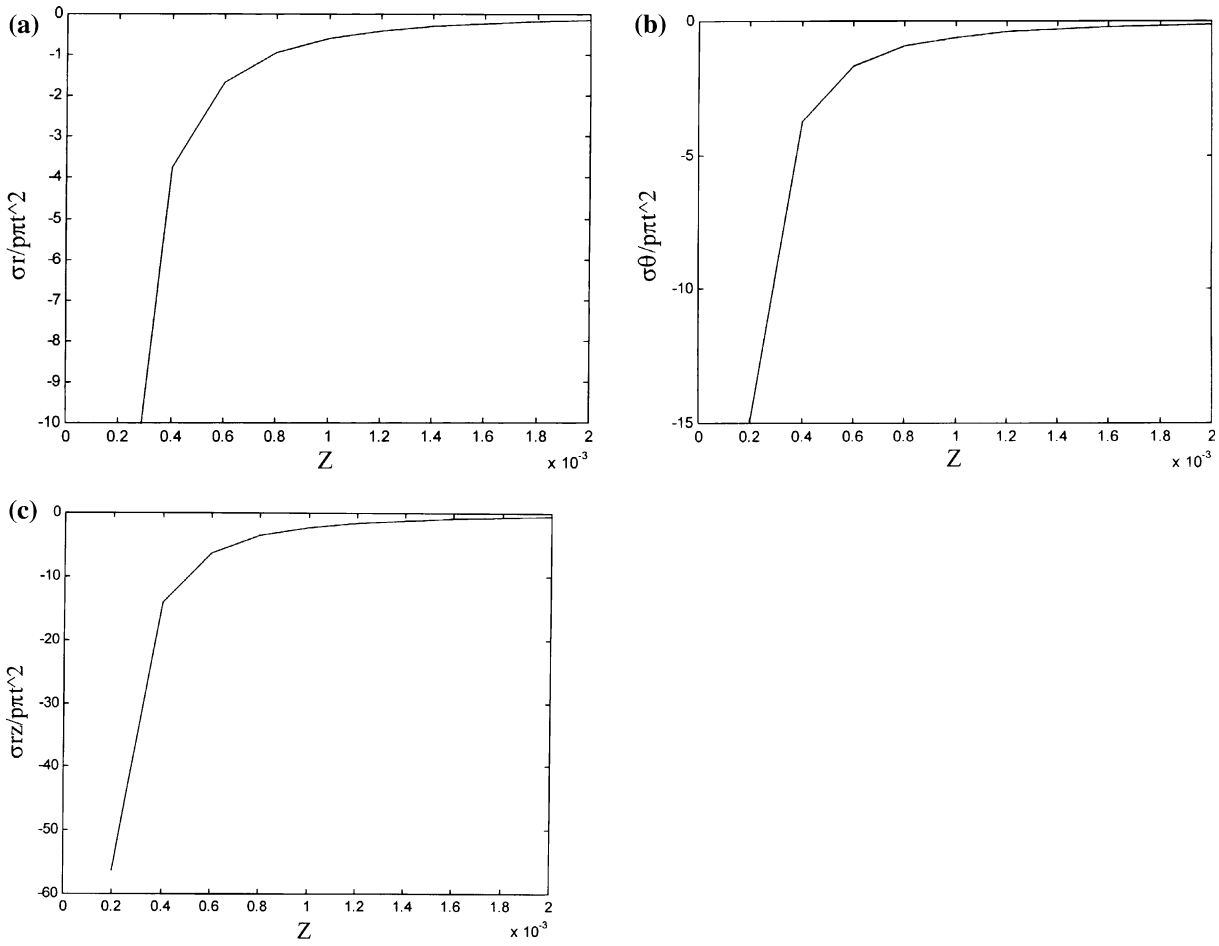

Fig. 3 (**a**) Variation in σ_r in the film along the depth. (**b**) Variation in σ_θ in the film along the depth. (**c**) Variation in σ_{rz} in the film along the depth

Poisson's ratio, as shown in Fig. 2a–c. The sinusoidal distribution in τ_{rz} in Fig. 2c shows the largest differences between peak values in all stress (σ_r, σ_θ, σ_z, τ_{rz}), which plays an important role in bonding properties.

The SEM or OM studies of indentation fracture of nitride/HSS and of nitride/SS system initially appear to be consistent with the elastic analysis. For fracture patterns next to the contact area, neither cracks nor spalling may be found for all nitride/SS as seen in Fig. 5c while there are some tiny radial cracks (Fig. 5a) for good bonding state and spalling (Fig. 5b) for poor bonding state in nitride/HSS. The cross-section views of indentation patterns show even more clearly the differences between these two systems. Inside the contact area, ring cracks, lateral cracks and spalling occur apparently in most nitride/SS specimens shown in Fig. 6a, whereas a much smoother indent surface without marked cracks occurs in nitride/HSS shown in Fig. 6b. The preceding elastic analysis can help explain these differences in indentation patterns. Among the stresses, the shear stress ($\tau_{rz} = \sigma_{rz}$) at the interface is expected to be the most important factor. Figure 2c shows that shear stress is symmetrical. The maximum stress is located at a distance to the load center (origin of coordinate) and the difference between the positive and negative maximum shear stresses becomes more significant with increasing Poisson's ratios (ν = 0.3~0.35 for SS [22]).The larger amount of cracks inside the indent cavity of nitride/SS appear to be consistent with the elastic calculations. Furthermore, calculation of σ_r and σ_θ (Fig. 2a, b) show that the differences in coating and substrate stress increase with increasing Poisson's ratios of the substrates, which facilitate the formation of ring cracks in the film surface in nitride/SS system.

Elastic/plastic analysis

The elastic analysis of stresses distribution cannot be all satisfactory, and it is reasonable to take the analysis a step further by taking into account the plastic deformation. In tensile test, as the steel is plastically stretched, the transverse cracks develop on the hard

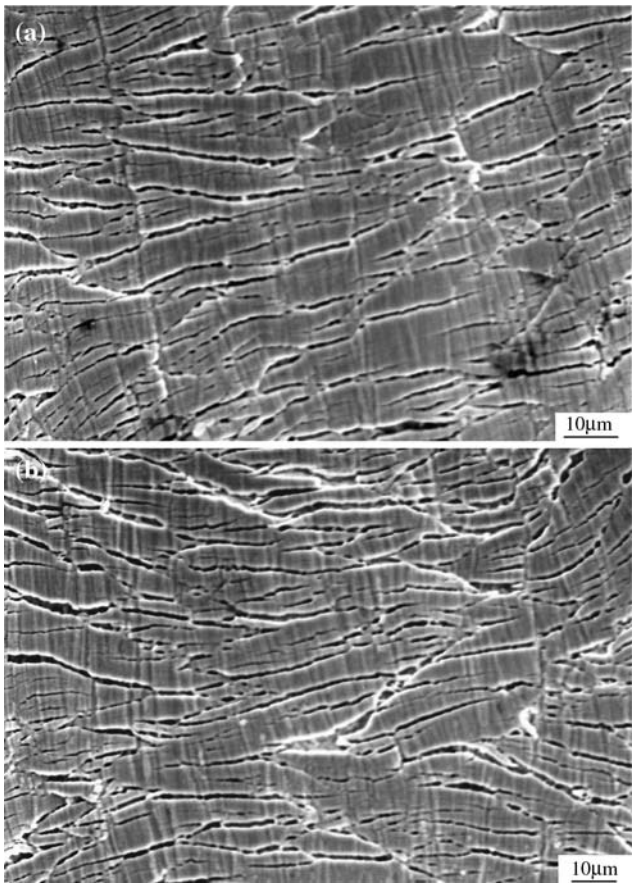

Fig. 4 (**a**) Fracture patterns of the film of TiN/SS after tensile test. (**b**) Fracture patterns of the film of TiN/HSS after tensile test

film as schematically explained by Agrawal [17]. The bonding differences between nitride/SS (σ_y = 430 MPa, v = 0.3~0.35 for SS [22]) and nitride/HSS (σ_y = 820 MPa, v = 0.2~0.23 for HSS [22]) can be distinguished by examining the tensile cracks on nitride films. Furthermore, the maximum shear stresses (τ_{max}), induced at the interface during tensile test, are evaluated by measuring crack spacings in the film and Eqs. 16 and 17, showing that the τ_{max} for TiN/HSS and TiN/SS are 1.61 MPa and 0.83 MPa, respectively (where λ (μ), ε_f (%), σ_f (GPa), k and $\delta(\mu)$ are 11.2, 0.72, 2.88, π, 2 and 15.6, 0.55, 2.2, π, 2 for TiN/HSS and TiN/SS, respectively). The result indicates that the interfacial bonding strength for TiN/HSS is higher than that for TiN/SS by the elastic/plastic model of Agrawal.

Stress concentration effect

The effect of stress concentration on the bonding quality in ceramic/metal system is rarely examined.

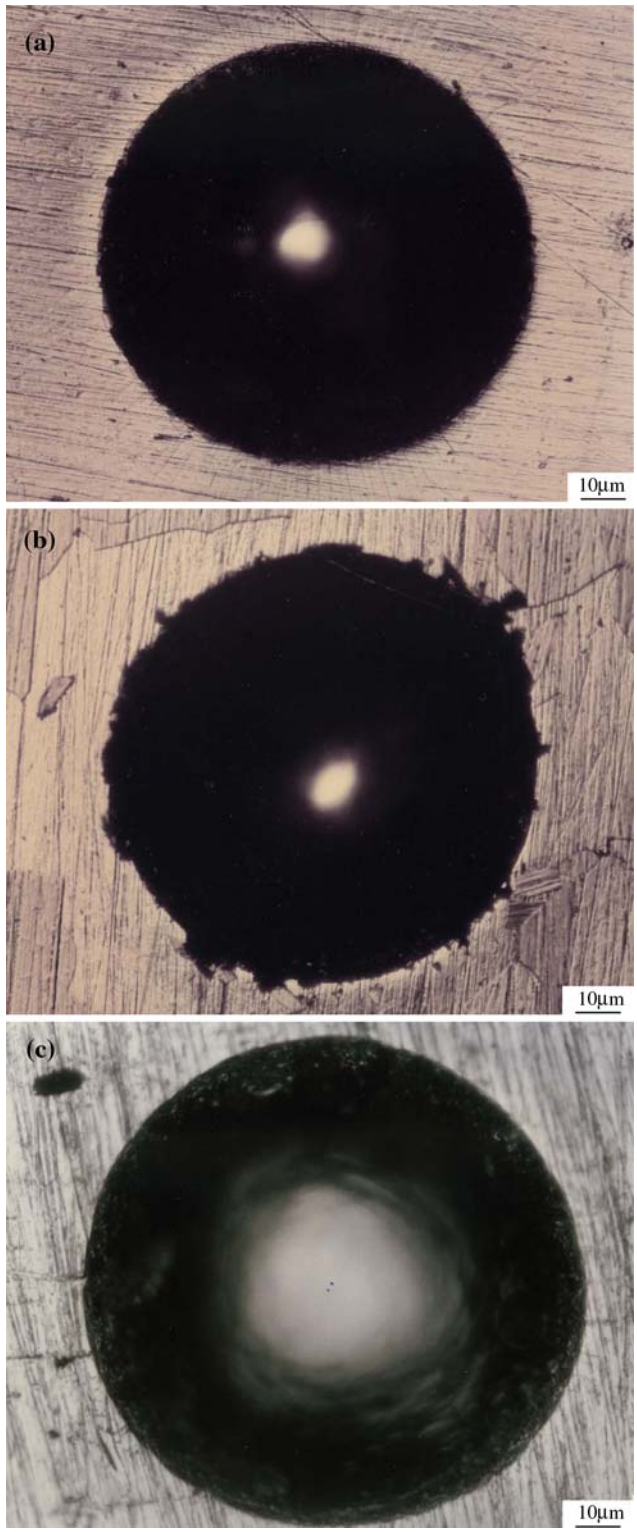

Fig. 5 (**a**) Indentation pattern of TiN/HSS with 220 watt power input, 15 min pre-sputtering and 150 kg indentation load. (**b**) Indentation pattern of TiN/HSS with 220 watt power input, 5 min pre-sputtering and 150 kg indentation load. (**c**) Indentation pattern of TiN/SS with 220 watt power input, 15 min pre-sputtering and 150 kg indentation load

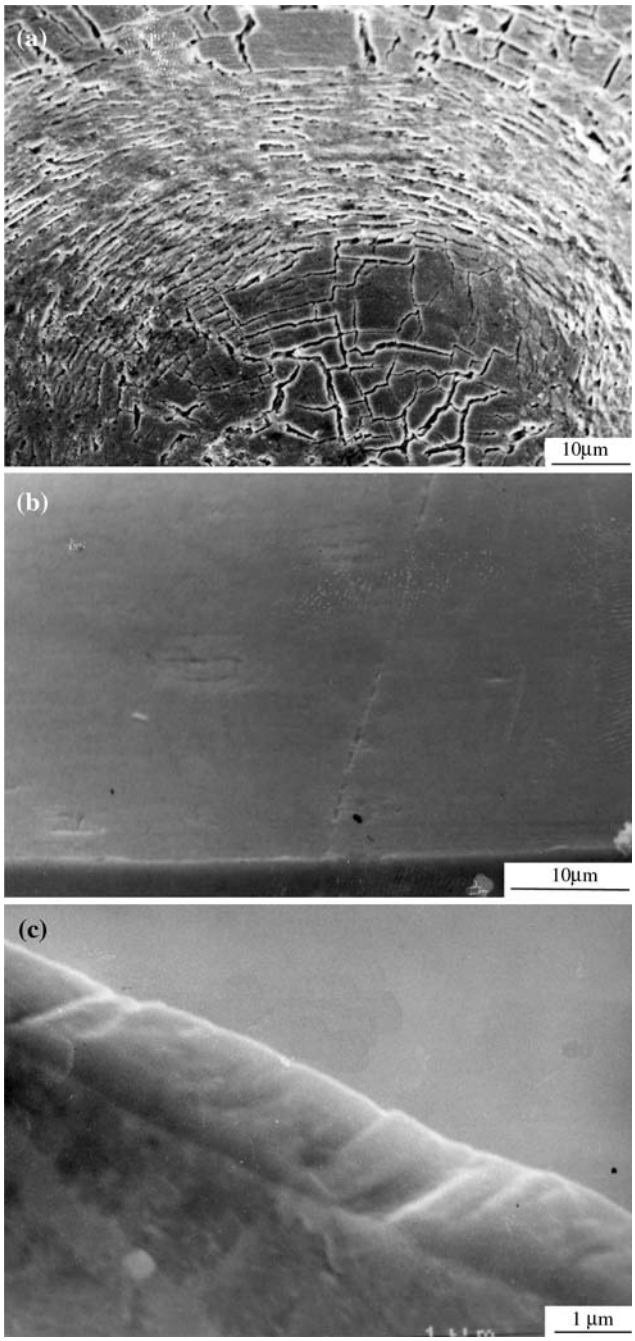

Fig. 6 (**a**) SEM image of the cross-section of indentation pattern of TiN/SS with 220 watt power input, 15 min pre-sputtering and 150 kg indentation load. (**b**) SEM image of the cross-section of indentation pattern of TiN/HSS with 220 watt power input, 15 min pre-sputtering and 150 kg indentation load. (**c**) SEM image of the cross-section of indentation pattern of TiN/HSS with 220 watt power, 15 min pre-sputtering and 150 kg indentation load, showing the strained (inclined) columnar structure

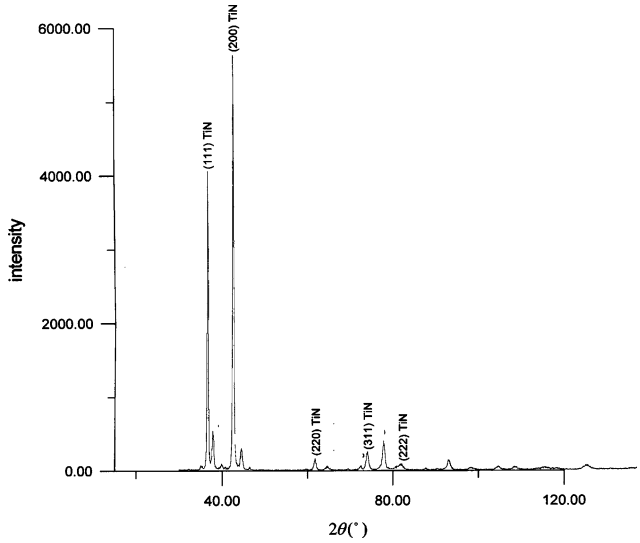

Fig. 7 XRD results for identifying the phases of TiN on steels

The difference in indentation fracture behavior between nitride/HSS and nitride/SS may be further explained by an additional parameter of stress concentration which is created at the edge, flaw tip and interface by the induced elastic stress and local residual stress by indention and uniform residual stress by the deposition process [23]. Compared with that of nitride/HSS system, the substrate of nitride/SS possesses higher Poisson's ratio and lower yield strength, and the larger plastic strain may cause the extension of ring cracks and lateral cracks and may introduce the stress concentration as the cracks approach the interface [24]. Figure 3a–c show that the stresses increase toward the interface during indenting, and the increase becomes larger with higher Poisson's ratio, thus causing more cracks and spallings. The effect of metallic plasticity on the growth of cracks from a flaw located in the ceramic adjacent to the interface can be analyzed combined with the theory of Evans [13]. It showed that the stress concentration increased as the flaw approaches the interface or the σ_y of the metal decreased. Substrate having low yield strength would inhibit decohesion by blunting film cracks at the interface [14]; however, the hard films on softer metal thus tended to fragment with remaining attached to the substrate. The shear lag approach provided a solution to the problem of fragmentation of adherent brittle films on a ductile substrate. The analysis indicated that spacing between fragments increased in direct proportion with the film thickness and increased in inverse proportion with the substrate yield stresses [15]. The critical forces for onset of plastic deformation of metal substrate and for coating fracture were also evaluated by finite element method (FEM) [16], it was found that high substrate yield strength and

lower Poisson's ratio help to achieve critical loads. From these results, it appears reasonable that the ring cracks, lateral cracks, and spallings inside the indented cavity of nitride/SS come from the larger sinusioidal shear stress due to the higher Poisson's ratio of SS and the plastic deformation due to the lower yield stress of SS which induces more local residual stress.

For the nitride/HSS system with much less plastic deformation, some cracks or spalling observed around the cavity come from the edge (bending) effect when the conical indenter strains the surface downward [24, 25]. The accumulated strain energy is not released gradually with cracking or spalling inside the cavity as the nitride/SS system, but is released only by the cracking or spalling around the cavity due to edge (bending) effects. The median radian cracks and lateral cracks also develop due to poor adherence of coating and are affected by the geometry of the indenter [9, 10]. It is expected that the stress concentration at the edge of cavity increases with decreasing radius. Accordingly, the edge effect becomes the dominant mode of failure in hard film/HSS system during indentation.

Conclusions

Different indentation fracture modes are observed between nitride/HSS and nitride/SS. The cracks or spalling or fragments appear next to the indentation contact area for nitride/HSS, but are found inside the indentation cavity for nitride/SS. The values of σ_r, σ_θ, σ_{rz} at the interface of nitride/SS are larger than those of nitride/HSS by elasticity analysis due to the larger stress concentration and residual stress in the nitride films next to the interface and the lower yield stress of substrate (SS). It is found that the major cause of the indentation fracture of nitride/SS is attributed to the Poisson's ratio effect, while that of nitride/HSS is due to the edge (bending) effect.

References

1. Lawn BR, Swain MV (1975) J Mater Sci 10:113
2. Lawn BR, Evans AG, Chantikul P (1979) J Mater Sci 14:2225
3. Lawn BR, Evan AG, Marshall DB (1980) J Am Ceram Soc 63:574
4. Marshall DB, Lawn BR, Evans AG (1982) J Am Ceram Soc 65:561
5. Mehrotra K, Quinto DT (1985) J Vac Sci Technol A 3:2401
6. Gruninger MF, Lawn BR, Farabaugh EN (1987) J Am Ceram Soc 70:344
7. Hu MS, Thouless MD, Evans AG (1988) Acta Metall 36:130
8. Sebastian S, Biswas SK (1991) J Phys D Appl Phys 24:113
9. Diao DF, Kato K, Hokkirigawa K (1994) J Tribol 116:860
10. Ogilvy JA (1993) J Phys D Appl Phys 26:2123
11. Heinke W, Leyland A, Matthews A, Berg G, Friedrich C, Broszeit E (1995) Thin Solid Films 270:431
12. Palmers J, Stappen MV, Haen JD, Olieslaeger MD, Stals LM, Uhlig G, Foller M, Haberlin E (1995) Surface Coating Technol 74–75:162
13. Evans AG, Lu MC, Schmauder S, Ruhle M (1986) Acta Metall 34(8):1643
14. Dalgleish BJ, Lu MC, Evans AG (1988) Acta Metall 36(8):2029
15. Hu MS, Evans AG (1989) Acta Metall 37(3):917
16. Michler J, Blank E (2001) Thin Solid Films 381:119
17. Agrawal DC, Raj R (1989) Acta Metall 37(4):1265
18. Shieu FS, Raj R, Sass SL (1990) Acta Metall 38(11):2215
19. Aitshulin S, Rosen A (1993) J Mater Sci 28:3749
20. Zhang S, Zhu W (1993) J Mater Process Technol 39:165
21. Kohayashi A (2000) Surface Coating Technol 132:152
22. Olivo CT (1987) In: Machine tool technology and manufacturing process. Albany, p 536
23. Drory MD, Thouless MD, Evans AG (1988) Acta Metall 36(8):2019
24. Thouless MD, Evans AG, Ashby MF, Hutchinson JW (1987) Acta Metall 35:1333
25. Rother B, Dietrich DA (1994) Thin Solid Films 250:81